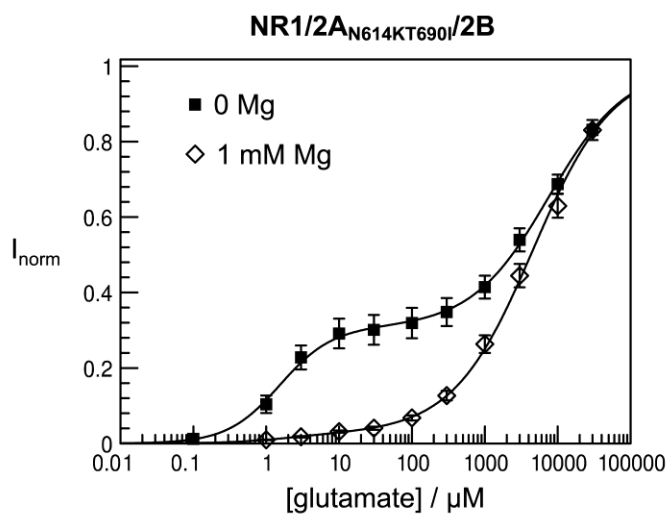
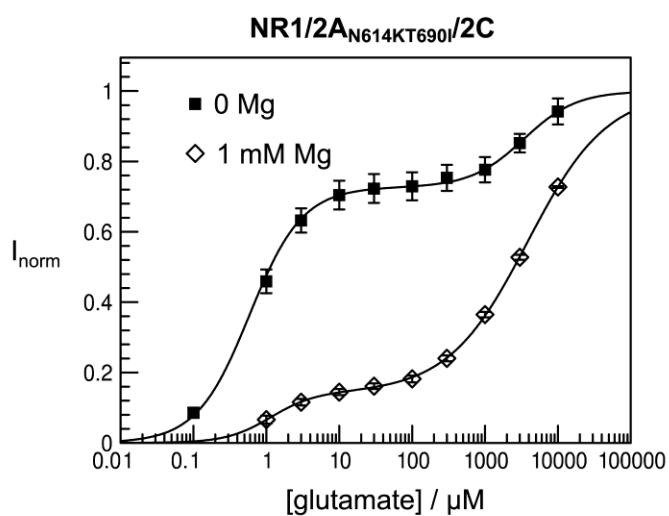
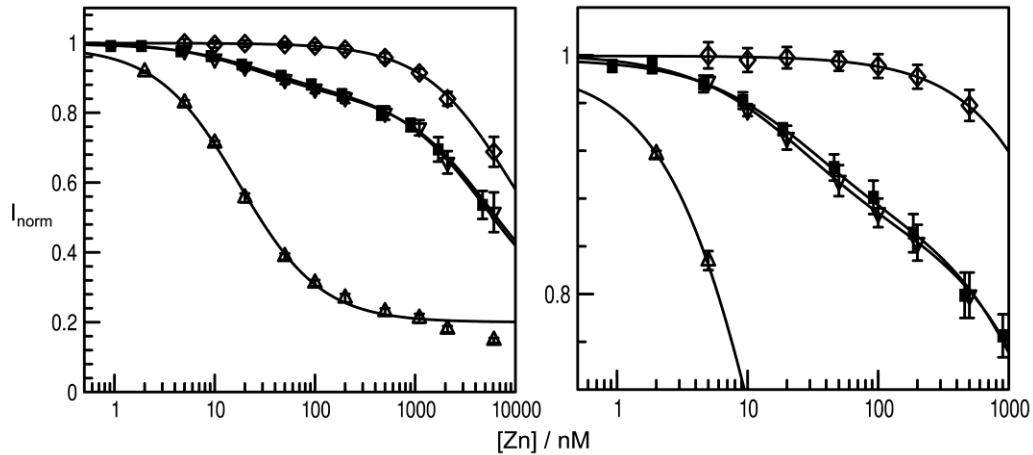


A**B**

Supplementary Figure 1: Pharmacological isolation of NR1/2A/2B and NR1/2A/2C triheteromeric NMDA receptors

(A) Glutamate concentration-response curves for oocytes expressing NR1, NR2A_{N614KT690I} and NR2B subunits and recorded in the absence (solid squares) or presence (open diamonds) of 1 mM Mg. Each point shows the average response from 4-10 cells. In the absence of Mg two components are readily distinguished; the first component has an affinity identical to that of NR1/2B wt receptors ($EC_{50} = 1.5 \pm 0.4 \mu\text{M}$, relative area = $30.7 \pm 0.3 \%$, $n_H = 1.21 \pm 0.17$) while the second has an affinity intermediate between that of NR1/2B wt and all-mutant NR1/NR2A_{N614KT690I} receptors (see Fig.2) and corresponds to the triheteromeric NR1/2A_{N614KT690I}/2B receptors ($EC_{50} \sim 7.5 \text{ mM}$, relative area = $69.3 \pm 15 \%$, $n_H = 0.82 \pm 0.23$). In the presence of 1 mM Mg, the NR1/2B wt component is almost completely abolished (relative area = $2.6 \pm 1.2 \%$) leaving an almost pure triheteromeric receptor population ($EC_{50} = 4.6 \pm 1.9 \text{ mM}$, relative area = $97.4 \pm 12.7 \%$, $n_H = 0.79 \pm 0.11$). **(B)** Glutamate concentration-response curves for oocytes expressing NR1, NR2A_{N614KT690I} and NR2C subunits and recorded in the absence (solid squares) or presence (open diamonds) of 1 mM Mg. Data are from 3-12 cells. In the absence of Mg two components are readily distinguished; the first component has an affinity identical to that of NR1/2C wt receptors ($EC_{50} = 0.6 \pm 0.1 \mu\text{M}$, relative area = $72.7 \pm 2.0 \%$, $n_H = 1.12 \pm 0.1$) while the second has an affinity intermediate between that of NR1/2C wt and all-mutant NR1/NR2A_{N614KT690I} receptors (see Fig.2) and corresponds to the triheteromeric NR1/2A_{N614KT690I}/2C receptors ($EC_{50} 3.4 \pm 2.3 \text{ mM}$, relative area = $27.3 \pm 8.1 \%$, n_H fixed = 1). In the presence of 1 mM Mg, the NR1/2C wt component is markedly reduced, but not completely abolished ($EC_{50} = 1.1 \pm 0.2 \mu\text{M}$, relative area = $14.2 \pm 5.0 \%$, $n_H = 1.44 \pm 0.44$). The majority of current in the presence of Mg is carried by the triheteromeric receptor population ($EC_{50} = 3.8 \pm 0.5 \text{ mM}$, relative area = $85.8 \pm 8.3 \%$, $n_H = 0.79 \pm 0.23$). Error bars represent standard errors.



Supplementary Figure 2: The glutamate binding mutation NR2A_{T690I} has little effect on Zn inhibition via the NR2-NTDs

Shows data from Fig. 4B (see legend for details), with the Zn concentration-inhibition curve (in 1mM Mg at -80 mV) recorded from cells expressing NR1, NR2A and NR2A_{H128SN614K} subunits superimposed (∇ , n=13 cells). Under these recording conditions, approximately 90% of the current is carried by triheteromeric NR1/2A/2A_{H128SN614K} receptors (see Results). Note that this curve is almost identical to that recorded from NR1/2A/2A_{H128SN614KT690I} receptors (■) indicating that inclusion of the T690I glutamate binding mutation has little effect on Zn inhibition via the NR2A-NTD of the associated NR2A wt subunit. Right-hand panel shows a close-up of the inhibition of triheteromeric receptors in the nM range. Fitted parameters for ∇ were: $IC_{50} = 25.0 \pm 4.6$ nM, 5.6 ± 1.0 μ M, relative area 19.0 ± 1.4 %, 81.1 ± 1.4 %, n_H fixed = 1. Error bars represent standard errors.